Priority Brief

Cancer Immunology Research

Breast Cancer Neoantigens Can Induce CD8$^+$ T-Cell Responses and Antitumor Immunity

Xiuli Zhang[1], Samuel Kim[1], Jasreet Hundal[2], John M. Herndon[1], Shunqiang Li[3], Allegra A. Petti[2], Savas D. Soysal[1,4], Lijin Li[1], Mike D. McLellan[2], Jeremy Hoog[3], Tina Primeau[3], Nancy Myers[1], Tammi L. Vickery[5], Mark Sturmoski[1], Ian S. Hagemann[6], Chris A. Miller[2,3], Matthew J. Ellis[3,7], Elaine R. Mardis[2,3], Ted Hansen[6], Timothy P. Fleming[1], S. Peter Goedegebuure[1], and William E. Gillanders[1,8]

Abstract

Next-generation sequencing technologies have provided insights into the biology and mutational landscape of cancer. Here, we evaluate the relevance of cancer neoantigens in human breast cancers. Using patient-derived xenografts from three patients with advanced breast cancer (xenografts were designated as WHIM30, WHIM35, and WHIM37), we sequenced exomes of tumor and patient-matched normal cells. We identified 2,091 (WHIM30), 354 (WHIM35), and 235 (WHIM37) nonsynonymous somatic mutations. A computational analysis identified and prioritized HLA class I–restricted candidate neoantigens expressed in the dominant tumor clone. Each candidate neoantigen was evaluated using peptide-binding assays, T-cell cultures that measure the ability of CD8$^+$ T cells to recognize candidate neoantigens, and preclinical models in which we measured antitumor immunity. Our results demonstrate that breast cancer neoantigens can be recognized by the immune system, and that human CD8$^+$ T cells enriched for prioritized breast cancer neoantigens were able to protect mice from tumor challenge with autologous patient-derived xenografts. We conclude that next-generation sequencing and epitope-prediction strategies can identify and prioritize candidate neoantigens for immune targeting in breast cancer. *Cancer Immunol Res; 5(7); 516–23. ©2017 AACR.*

Downloaded from http://aacrjournals.org/cancerimmunolres/article-pdf/5/7/516/2351349/516.pdf by guest on 18 July 2024

Introduction

Next-generation sequencing technologies have transformed our understanding of how somatic mutations contribute to cancer initiation and progression. Improvements in instrument performance together with cost reductions have enabled a systematic analysis of the mutational landscape in a variety of cancer types. The results provide opportunities to personalize therapy. In preclinical models, cancer neoantigens can be identified by next-generation sequencing, and neoantigens can be prioritized by epitope prediction algorithms. Some neoantigens are targets for checkpoint blockade therapy and personalized vaccine therapy (1–3). Ongoing clinical trials confirm the importance of cancer neoantigens in the response to therapies based on immune checkpoint inhibitors or personalized vaccines in non–small cell lung cancer, melanoma, and colorectal cancers with DNA mismatch repair deficiency (4–9). Here, we explored neoantigens in breast cancer, which generally does not carry a high mutational load.

Materials and Methods

Human subjects

All human subjects' research was reviewed and approved by the Human Subjects Committee at Washington University School of Medicine. Three advanced-stage breast cancer patients participated in these studies. Each subject consented to tissue banking and establishment of patient-derived xenografts (PDX). PDXs were established in NSG mice (10) and early-generation tumors were flash frozen. Each subject also consented to leukapheresis. The subjects were designated WHIM30, WHIM35, and WHIM37 based on the designation of their PDX. Leukapheresis was performed at Barnes Jewish Hospital. Peripheral blood mononuclear cells (PBMC) were isolated through density centrifugation using Ficoll–Paque PLUS and cryopreserved as cell pellets. Each subject consented to genome sequencing. Aliquots of PBMCs were frozen as cell pellets. DNA from PDX tumors and PBMC was extracted using the QIAamp DNA Mini Kit (Qiagen Sciences) and RNA from PDX tumors was extracted using the High Pure RNA Paraffin kit (Roche). DNA and RNA quality was determined using a

[1]Department of Surgery, Washington University School of Medicine, St. Louis, Missouri. [2]McDonnell Genome Institute, Washington University School of Medicine, St. Louis, Missouri. [3]Department of Medicine, Division of Oncology, Washington University School of Medicine, St. Louis, Missouri. [4]Department of Surgery, University Hospital Basel, Basel, Switzerland. [5]Center for Human Immunology and Immunotherapy Programs, Washington University School of Medicine, St. Louis, Missouri. [6]Department of Pathology and Immunology, Washington University School of Medicine, St. Louis, Missouri. [7]Lester and Sue Smith Breast Care Center, Oncology/Medicine and MCB, Baylor College of Medicine, Houston, Texas. [8]The Alvin J. Siteman Cancer Center at Barnes-Jewish Hospital and Washington University School of Medicine, St. Louis, Missouri.

Note: Supplementary data for this article are available at Cancer Immunology Research Online (http://cancerimmunolres.aacrjournals.org/).

Corresponding Author: William E. Gillanders, Washington University in St. Louis, 660 South Euclid Avenue, St. Louis, MO 63110. Phone: 314-747-0072; Fax: 314-454-5509; E-mail: gillandersw@wudosis.wustl.edu

doi: 10.1158/2326-6066.CIR-16-0264

©2017 American Association for Cancer Research.

AACR

Nanodrop 2000 and quantitated using a Qubit Fluorometer (Life Technologies).

Exome sequencing

For each subject, tumor and normal matched DNA samples were processed for whole-exome sequencing using standard protocols for Kapa Biosystems NGS libraries with corresponding barcoded adapters. The libraries were quantitated and combined at equimolar ratios into an exome capture using the Roche Nimblegen EZ Exome version 3.0 reagent. Exome sequence data were generated as 2×100 bp read pairs on an Illumina HiSeq2000 instrument. Our Genome Modeling System (GMS; ref. 11) was used to align exome reads and identify somatic variants. The analysis pipeline uses BWA (version 0.5.9; ref. 12) for alignment with default parameters except for the following: −t 4 −q 5. All alignments were against GRCh37-lite-build37 of the human reference genome and were merged and subsequently de-duplicated with Picard (version 1.46). Detection of somatic mutations was performed using a combination of different variant callers, including SAMtools (13, 14), Somatic Sniper (15), VarScan Somatic (16, 17), and Strelka (18).

cDNA-capture sequencing

All RNA samples were DNase-treated with a TURBO DNA-free kit (Invitrogen) as per the manufacturer's instructions. RNA integrity and concentration were assessed using an Agilent Eukaryotic Total RNA 6000 assay (Agilent Technologies) and a Quant-iTTM RNA assay kit on a QubitTM Fluorometer (Life Technologies Corporation). The MicroPoly(A)PuristTM Kit (Ambion) was used to enrich for poly(A) RNA from three WHIM patients DNAse-treated total RNA, and the resulting RNA was converted to cDNA using the Ovation RNA-Seq System V2 (NuGen, 20 ng of either total or polyA RNA). All NuGen cDNA sequencing libraries were generated using NEBNext UltraTM DNA Library Prep Kit for Illumina as described previously (19). Each library ligation reaction was PCR-optimized using the Eppendorf Epigradient S qPCR instrument, and PCR-amplified for limited cycle numbers based on the Ct value identified in the optimization step. Libraries were quantitated using the Quant-iTTM dsDNA HS Assay (Life Technologies) and for size using the BioAnalyzer 2100 (Agilent Technologies). The Illumina-ready libraries were enriched using the Nimblegen SeqCap EZ Human Exome Library v3.0 reagent. Each hybridization reaction was incubated at 47°C for 72 hours, and single-stranded capture libraries were recovered and PCR-amplified per the manufacturer's protocol. Post-capture library pools were sized and purified with AmpureXP magnetic beads to remove residual primer dimers and to enrich for a library fragment distribution between 300 and 500 bp, then diluted to 2 nmol/L prior to Illumina paired-end sequencing. Paired-end reads were trimmed with flexbar v 2.21 (params: –adapter CTTTGTGTTTGA –adapter-trim-end LEFT –nono-length-dist –threads 4 –adapter-min-overlap 7 –max-uncalled 150 –min-readlength 25) to remove single primer isothermal amplification adapter sequences The resulting reads were analyzed with a pipeline that included Tophat v2.0.8 (params: –bowtie-version = 2.1.0 for Ovation; –library-type fr-firststrand – bowtie-version = 2.1.0 for Truseq; ref. 2). Expression levels (FPKM) were calculated with Cufflinks v2.0.2 (params–max-bundle-length=10000000–num-threads 4). cDNA capture data were reviewed visually to evaluate the expression of mutations identified by exome data and neoantigen prediction pipeline from pVacSeq. Both cDNA-capture (Alt-read number) and FPKM values were considered for candidate neoantigen prioritization.

HLA typing

The subject's HLA type was determined by PCR-SSOP (ProImmune).

Neoantigen identification

We developed a pipeline for the identification and prioritization of potential neoantigens resulting from the somatic missense mutations detected from exome sequencing analysis. Briefly, thresholds for filtering (binding- and coverage-based) using both the exome and cDNA-cap sequencing data detailed above were used to compile a list of expressed somatic missense mutations. Next, amino-acid substitutions corresponding to each of the coding missense mutations were translated into a 21-mer amino acid FASTA sequence, with 10 amino acids flanking the substituted amino acid on each side. For each patient, these 21-mer amino-acid sequences were evaluated through the HLA class I peptide–binding algorithm NetMHC v3.2 (20, 21) to identify high-affinity neoantigens predicted to bind with high affinity to the patient's HLA alleles. We similarly evaluated the corresponding wild-type sequences to compare differences in predicted binding affinities, wherein any candidate neoantigens with a predicted binding affinity IC_{50} value < 500 nm were considered for further evaluation. This pipeline evolved into the pVAC-Seq pipeline (2) pipeline for identification of candidate neoantigens.

Sanger sequencing of DNA samples

DNA of patient PBMCs: xenograft and parental tumor tissue was extracted with Qiagen QIAamp DNA Mini Kit and AllPrep DNA/RNA FFPE Kit, respectively. Primers were designed with Primer-3. PCR reactions were carried out in 20 μL with 40 ng of DNA according to the manufacturer's recommendation of Phusion High-Fidelity DNA Polymerase (ThermoFisher Scientific). PCR products were purified with QIAquick gel extraction (Qiagen) followed by sequencing (GeneWiz).

Peptides

Peptides were obtained lyophilized from Peptide 2.0 Inc. (>95% purity) and were dissolved in sterile water or in 10% DMSO dependent on the amino acid sequence.

Mice

NOD SCID gamma (NSG) mice were purchased from The Jackson Laboratory and housed in a specific pathogen-free animal facility. All *in vivo* experiments used 8- to 12-week-old female NSG mice. All studies were performed in accordance with procedures approved by the AAALAC-accredited Animal Studies Committee of Washington University in St. Louis.

Flow cytometry

The following anti-human monoclonal antibodies (mAb) were used for cell surface staining: CD3-APC-Cy7 (clone: OKT3), CD4-FITC (clone: OKT4), CD8-AF700 (clone: SK1), and CD45-BV785 (clone: HI30). All antibodies were obtained from BioLegend. Samples were analyzed on an LSR Fortessa flow cytometer (BD Biosciences), and data were analyzed using FlowJo software.

Downloaded from http://aacrjournals.org/cancerimmunolres/article-pdf/5/7/516/2351349/516.pdf by guest on 18 July 2024

Peptide binding assay

Binding of synthetic peptides was assessed by measuring induction of surface expression of HLA class I molecules: Peptide binding to several commonly expressed human class I alleles was determined using T2 cells and genetically modified T2 cells, specifically T2-A3 (kindly provided by Dr. Storkus from UPMC/UPC) and T2-B7 cells (kindly provided by Dr. Lutz, University of Kentucky). Following an established protocol (22) with a few modifications, peptides (100 μmol/L) were incubated with T2, T2-A3, or T2-B7 cells in serum-free RPMI at room temperature for 1 hour, then transferred to 28°C in a CO_2 incubator. The following day, cells were stained with HLA allele–specific mAb (anti–HLA-A2 (BD Pharmingen); anti–HLA-A3 (BD Pharmingen); and anti–HLA-B7 (provided by Dr. Ted Hansen), and analyzed by flow cytometry.

In vitro T-cell analysis

In vitro studies to evaluate the immunogenicity of candidate neoantigens was performed using patients' autologous PBMC. Briefly, PBMCs were cultured with individual peptides corresponding to candidate neoantigens at 50 μg/mL in RPMI with 5% human serum, 10 units/mL penicillin–streptomycin, 10 mmol/L HEPES buffer, 2 mmol/L L-glutamine, 1 × nonessential amino acid. IL2 (50 U/mL) was added every 2 days. Control PBMCs were stimulated with peptides corresponding to known viral antigens. On day 12, the peptide and tumor reactivity of the T cells was determined by IFNγ ELISPOT assay. Cultured T cells were stimulated with peptide pulsed or autologous tumor-pulsed, irradiated autologous PBMC in the ELISPOT plate followed by 20-hour incubation at 37°C. Developed spots were counted in an ELISPOT reader (C.T.L.). In a different set of experiments, patients' PBMCs were cultured with irradiated autologous tumor cells instead of neoantigens for 12 days, as above. Tumor-primed T cells were tested for recognition of neoantigens by IFNγ ELISPOT assay.

In vivo T-cell analysis

PDX tumor cells were subcutaneously injected into immunodeficient NSG mice (1×10^6 cells per mouse). When tumors became palpable (around 3–4 mm in dimension), 5×10^6 PBMCs stimulated with prioritized neoantigens or control viral antigens were transferred weekly into tumor-bearing NSG mice through tail-vein injection (23–25). Mice were observed daily and tumor size was measured every 2 days. In selected cases, PDX tumor–bearing NSG mice were sacrificed at 30 days, and peripheral blood and tumor were harvested from each mouse. Tumor tissue was processed into a single-cell suspension through mechanical (Miltenyi gentle MACS) and enzymatic dissociation followed by filtration through a 70 μmol/L cell strainer. The single-cell suspension and PBMCs were stained for immune subsets followed by flow cytometry. Functional analysis was performed by the IFNγ ELISPOT assay using neoantigen peptides identified from each patient.

Statistical analyses

Samples were compared using an unpaired, two-tailed Student *t* test, unless specified.

Results

To determine whether breast cancer neoantigens can be targeted with immunotherapy, we established patient-derived xenografts from 3 patients with advanced breast cancer, designated WHIM30, WHIM35, and WHIM37 (Supplementary Table S1 and Supplementary Fig. S1). We sequenced tumor and normal whole exomes and identified 2091 (WHIM30), 354 (WHIM35), and 235 (WHIM37) nonsynonymous single-nucleotide variant (SNV) mutations using a published somatic variant pipeline (Table 1; Supplementary Tables S2–S4; ref. 11). We filtered the results of this pipeline analysis using stringent criteria for tumor and normal read coverage, applying a minimal variant allele frequency (VAF) of 40%. This filter prioritized 74 (WHIM30), 33 (WHIM37), and 55 (WHIM37) candidate neoantigens from the dominant tumor clone of the patient-derived xenografts. We next examined cDNA-capture sequencing from the tumor RNA (3), to confirm that each mutant allele that was identified by our DNA-based analysis was expressed in RNA, and to exclude any gene represented at fewer than 1 fragment per kilobase of transcripts per million mapped reads (FPKM; Supplementary Table S5). We also generated HLA typing data for each patient using PCR-SSOP (Supplementary Table S6). We selected nonsynonymous SNV mutations with a predicted binding affinity to the restricting HLA alleles of <500 nmol/L. The final prioritized candidate neoantigens and their corresponding peptide sequences (Supplementary Tables S7–S9) were pursued for further study.

Peptides corresponding to the candidate neoantigens were synthesized and assessed for binding to the corresponding HLA class I allele using T2 cells (HLA-A02:01), and genetically modified T2 cells expressing HLA-A03:01 or HLA-B07:02 (26). Of the 18 peptides tested, 15 (83%) bound to the predicted HLA allele (Table 1; stabilization of MHC expression was measured by flow cytometry, Supplementary Fig. S2). To evaluate the ability of autologous T cells to recognize the candidate neoantigens *in vitro*, we cocultured peptides corresponding to the candidate neoantigens with corresponding autologous PBMCs for 12 days in the

Table 1. Overview of identified neoantigens

Patient	Number of tier 1 mutations[a]	Number of mutations expressed[b]	Number predicted to bind[c]	Number actually binding/tested[d]	Number immunogenic *in vitro*[e]	Number conferring tumor recognition[f]
WHIM30	2,091	15	9	7/8	2/9	2/2
WHIM35	354	8	8	3/3	1/7	1/1
WHIM37	235	11	8	6/8	1/8	1/1

[a]As determined by whole-exome sequencing and from each patient xenograft.
[b]As determined by cDNA Cap-Seq and other filters described in Materials and Methods.
[c]As determined by NetMHC 3.2 (affinity of mutant peptides < 500 nmol/L).
[d]Binding assay evaluated using the T2 assay.
[e]Reactivity as determined by IFNγ ELISPOT assay *in vitro* as described in Materials and Methods.
[f]Reactivity as determined by tumor growth inhibition in the NSG mouse model *in vivo* as described in Materials and Methods.

Downloaded from http://aacrjournals.org/cancerimmunolres/article-pdf/5/7/516/2351349/516.pdf by guest on 18 July 2024

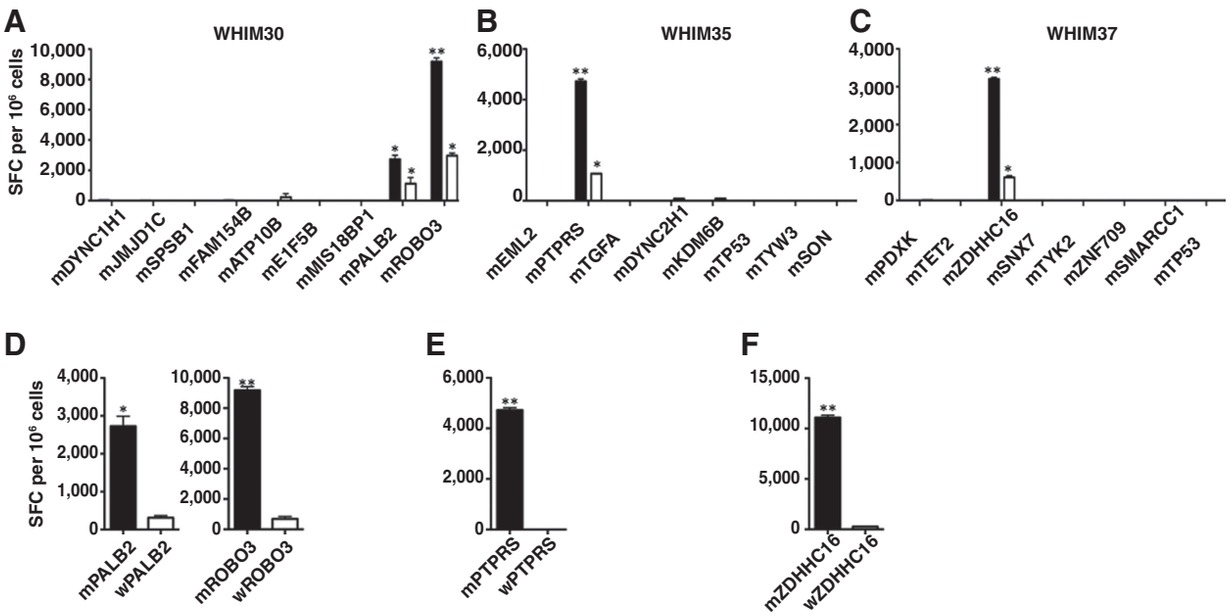

Figure 1.

Identification and validation of candidate neoantigens. Autologous PBMCs were stimulated with candidate breast cancer neoantigens for 12 days. $CD8^+$ T-cell IFNγ ELISPOT assays were performed on day 12 by coculturing stimulated PBMCs overnight with autologous, irradiated PBMCs pulsed with the candidate neoantigens (black) or irradiated PDX tumor cells (white). The immune response induced by candidate neoantigens and PDX tumor cells is shown in (**A**) WHIM30, (**B**) WHIM35, and (**C**) WHIM37. Negative controls in the ELISPOT assays included responder T cells cultured with no peptide (number of spot-forming cells per 10^6 cells was 50–120) or irrelevant peptide (number of spot-forming cells per 10^6 cells was 250–400). The background with irrelevant peptide was subtracted from the experimental condition in each case. To confirm the specificity of the immune response induced by candidate neoantigens, $CD8^+$ T-cell IFNγ ELISPOT assays were performed against mutant (black) and wild-type peptides (white) after 12-day stimulation with mutant peptides. The results are shown in (**D**) WHIM30, (**E**) WHIM35, and (**F**) WHIM37. Data are presented as means ± SEM ($n = 3$ wells per peptide in ELISpot assay) and are representative of three independent experiments. Samples were compared using unpaired, two-tailed Student test (*, $P < 0.05$; **, $P < 0.01$); SFC, spot-forming cells.

presence of IL2, after which the T-cell response to each peptide was assessed in an IFNγ ELISPOT assay. Two of nine (22%) WHIM30 candidate neoantigens (PALB2 and ROBO3) induced significant peptide-specific T-cell responses (*, $P < 0.05$; **, $P < 0.01$, respectively; Table 1; Fig. 1A). One of eight (12.5%) WHIM35 candidate neoantigens (PTPRS), and one of eight (12.5%) WHIM 37 candidate neoantigens (ZDHHC16) also induced significant peptide-specific $CD8^+$ T-cell responses (*, $P < 0.05$; **, $P < 0.01$, respectively; Table 1; Fig. 1B and C). The same candidate neoantigens induced 1.6–3 times increased $CD8^+$ T-cell responses compared with control peptides after autologous mixed lymphocyte–tumor cultures using PBMC and irradiated PDX-tumor cells (Supplementary Fig. S3).

To further characterize the specificity of the T-cell response to the prioritized breast cancer neoantigens, we stimulated each patient's PBMC with peptides corresponding to the mutant antigens for 12 days, then measured response to the antigens by IFNγ ELISPOT assays. Mutant PALB2-stimulated T cells did not cross-react with wild-type PALB2 (Fig. 1D). A similar pattern of reactivity was observed with the other breast cancer neoantigens: mutant, but not wild-type, ROBO3 (Fig. 1D), PTPRS (Fig. 1E), and ZDHHC16 (Fig. 1F) induced T-cell responses. These T-cell responses were not cross-reactive with the corresponding wild-type antigens. The recognition of mutant antigens was HLA restricted, as both allele-specific and HLA class I framework antibodies significantly reduced IFNγ secretion (*, $P < 0.05$; **, $P < 0.01$, respectively; Supplementary Fig. S4).

Two breast cancer neoantigens, PTPRS and ZDHHC16, are HLA-A02:01 restricted. We tested the immunogenicity of these neoantigens in HHD mice. HHD mice are transgenic for a mutant form of HLA-A2:01 that can interact with murine CD8 molecules, but they lack murine MHC class I alleles. HHD mice were immunized with mutant PTPRS or ZDHHC16 peptide plus poly I:C. The neoantigen-specific T-cell response was then measured by IFNγ ELISPOT. The mutant PTPRS and ZDHHC16 peptides, but not other HLA-A02:01-specific breast cancer neoantigens, induced a 3 to 6 times increasedneoantigen-specific immune response (Supplementary Fig. S5).

To assess whether neoantigen-specific $CD8^+$ T cells can recognize tumors, PBMCs cultured *in vitro* in the presence of mutant peptides were tested for reactivity against autologous tumor cells in IFNγ ELISPOT assays. Both PALB2- and ROBO3-specific T cells (WHIM30) recognized WHIM30 tumor cells (Fig. 1A). Similarly, PTPRS-specific T cells (WHIM35) and ZDHHC16-specific T cells (WHIM37) recognized WHIM35 and WHIM37 tumor cells, respectively (Fig. 1B and C). In contrast, PBMC cultured with control peptides, including an immunogenic peptide derived from mammaglobin-A (27), an immunodominant viral peptide, or EML2, an HLA-A02:01–binding but nonimmunogenic mutant peptide (WHIM30), did not recognize tumor cells. PBMCs stimulated with control peptides were responsive to the control peptides, except peptide EML2, which is a nonimmunogenic neoantigen. Thus, neoantigen-specific $CD8^+$ T cells do recognize their cognate tumors.

Downloaded from http://aacrjournals.org/cancerimmunolres/article-pdf/5/7/516/2351349/516.pdf by guest on 18 July 2024

Breast cancer neoantigens might be useful as targets for personalized cancer vaccines or other immunotherapeutic strategies. Here, we assessed whether neoantigen-specific $CD8^+$ T cells are associated with antitumor immunity *in vivo*. We began by implanting WHIM30 tumor sections subcutaneously in immune-compromised NOD SCID gamma (NSG) mice. After tumors became palpable, 5×10^6–10×10^6 autologous PBMC stimulated *in vitro* with PALB2, ROBO3 or control CMV peptides were adoptively transferred into tumor-bearing mice. Adoptive transfer was repeated every 7 days. Tumor growth was measured every 2 days. Adoptive transfer of autologous PBMC stimulated with PALB2 and ROBO3 was associated with decreased tumor growth, whereas adoptive transfer of PBMC stimulated with CMV had no impact on tumor growth (Fig. 2A and C). Adoptive transfer of autologous PBMC from patient WHIM35 stimulated *in vitro* with PTPRS

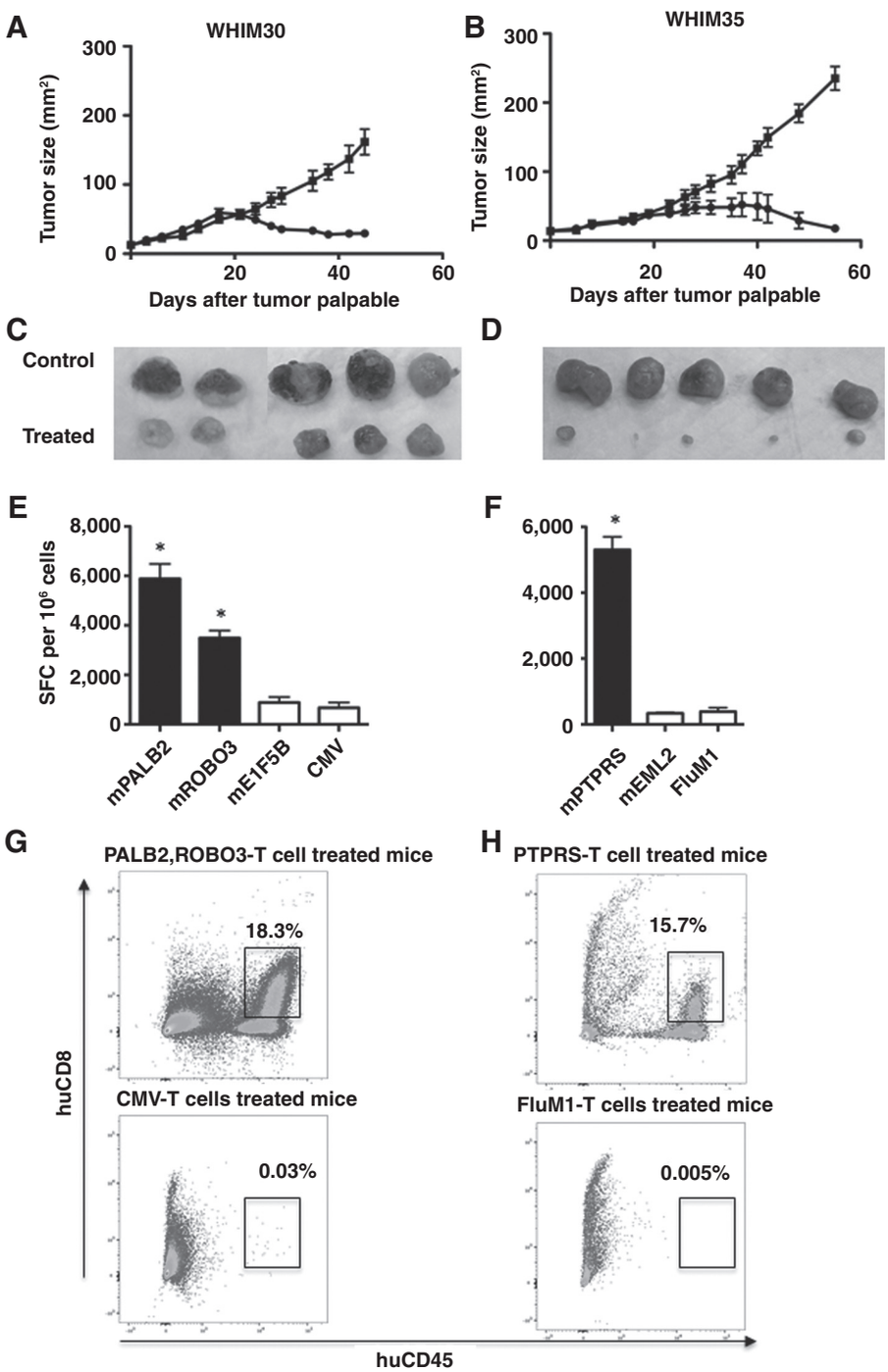

Figure 2.

Adoptive transfer of neoantigen-stimulated T cells inhibits growth of PDXs *in vivo*. PDXs were established by injection of 1×10^6 tumor cells subcutaneously into NSG mice. A total of $5–10 \times 10^6$ neoantigen-stimulated T cells and control viral-antigen stimulated T cells were adoptively transferred into tumor-bearing mice after the tumor became palpable. T cells were transferred at days 0, 7, and 14. Tumor size was measured every 2 days. **A,** WHIM30 tumor growth following treatment with PBMC stimulated with mutant PALB2/ROBO3 (black solid circle) or CMV peptides (black solid square). **B,** WHIM35 tumor growth following treatment with PBMC stimulated with mutant PTPRS (black solid circle) or FluM1 peptides (black solid square). **A** and **B,** Data are presented as tumor size (mm^2) ± SEM of 5 mice per group (*, $P < 0.05$). **C,** WHIM30 tumor size (52 days after tumor challenge) following treatment with PBMCs stimulated with mutant PALB2/ROBO3 or CMV peptides. **D,** WHIM35 tumor size (62 days after tumor challenge) following treatment with PBMCs stimulated with mutant PTPRS or CMV peptides. **E** and **G,** TILs were isolated from WHIM30 tumors following treatment with PBMC stimulated with mutant PALB2/ROBO3 (black) or negative control mutant E1F5B and CMV (white) peptides. $CD8^+$ T-cell IFNγ ELISPOT assay and flow cytometry were performed with experimental and control peptides as indicated. **F** and **H,** TILs were isolated from WHIM30 tumors following treatment with PBMC stimulated with mutant PTPRS (black) or negative control mutant EML2 and FluM1 peptides (white). $CD8^+$ T-cell mIFNγ ELISPOT assay and flow cytometry were performed with experimental and control peptides as indicated. **E** and **F,** Data shown are mean ± SEM ($n = 3$ wells per peptide in ELISpot assay). Data shown are representative of three independent experiments. Samples were compared using an unpaired, two-tailed Student *t* test ($P < 0.05$).

Downloaded from http://aacrjournals.org/cancerimmunolres/article-pdf/5/7/516/2351349/516.pdf by guest on 18 July 2024

but not FluM1 peptide decreased WHIM 35 tumor growth ($P < 0.05$; Fig. 2B and D).

To understand the mechanism of action of tumor rejection following adoptive transfer, we isolated tumor-infiltrating lymphocytes (TIL) from rejecting tumors and assayed them *ex vivo* by IFNγ ELISPOT. TILs from rejecting WHIM30 tumors generated IFNγ in response to both mPALB2 and mROBO3 (Fig. 2E). TILs from rejecting WHIM 35 tumors generated IFNγ in response to mPTPRS (Fig. 2F). In both cases, no response to control peptides was observed. Phenotypic analysis of TIL confirmed the presence of neoantigen-stimulated T cells in rejecting tumors. In contrast, no T cells were detectable in growing tumors following the adoptive transfer of control, viral antigen-stimulated T cells (Fig. 2G and H).

Sanger sequencing results showed that the PTPRS mutation (G to A) was present in the WHIM35 parental tumor as well as in the WHIM35 PDX tumor, but not in the patient's PBMC. DNA degradation in parental WHIM 30 and WHIM37 tumors prevented detection of neoantigens.

Discussion

We have used next-generation sequencing and computational analysis to identify and prioritize candidate breast cancer neoantigens. Some of these candidate neoantigens were recognized by the immune system, thus presenting potential targets for cancer immunotherapy. Successful design of precision vaccines for treatment of human cancer will depend on rapid identification and prioritization of candidate neoantigens (1–4, 28–30). Based on the data presented here, we have initiated two phase I clinical trials testing neoantigen DNA and synthetic long-peptide vaccines in patients with triple-negative breast cancer (TNBC; NCT02348320 and NCT02427581, respectively).

TNBC lacks expression of estrogen receptor, progesterone receptor, and HER2 and follows an aggressive clinical course. Clonal and mutational analysis of primary TNBC suggests that TNBC is characterized by a higher mutational frequency than other breast cancer subtypes (31–33). The relative abundance of somatic mutations in TNBC suggests that neoantigens are more likely to be present in this breast cancer subtype. Here, we observed that WHIM30, derived from a patient with TNBC, had over 2000 somatic mutations. We identified and credentialed two candidate neoantigens using algorithms designed to prioritize neoantigens from the dominant tumor clone, followed by *in vitro* and *in vivo* immune assays. WHIM35 and WHIM37 are luminal subtype breast cancers, with correspondingly lower mutational loads than WHIM30. Nonetheless, we identified and credentialed neoantigens in both these tumors, consistent with recent reports that human tumors containing limited mutations harbor neoantigens that can be targeted by immune therapies (34).

The limited number of neoantigens identified in TNBC may be a shortcoming of our identification process or may be related to the underlying biology of TNBC. Our sequencing and epitope prediction algorithms are similar to those of other investigators: we identified somatic missense mutations through exome sequencing of tumor and normal tissue, followed by expression analysis by RNA sequencing, as many mutations are not expressed. Our final step toward identification of candidate neoantigens involved the use of computer algorithms that predict which mutations can give rise to peptides that can be presented by the patient's HLA alleles (30, 35, 36). Preclinical studies performed to date suggest that the majority of candidate neoantigens, i.e., those that are expressed and predicted to bind with high affinity, do not trigger detectable T-cell responses. For example, of the top 62 predicted binding epitopes, only 2 conferred tumor rejection in a mouse sarcoma model (1). Likewise, Verdegaal and colleagues (37) identified 501 and 226 nonsynonymous mutations in two patients with advanced melanoma, respectively, but only 2 of 501 and 3 of 226 triggered antigen-specific $CD8^+$ T cells. Relevant data from human breast cancers are not readily available. In the studies presented here we validated one or two neoantigens per patient out of eight to nine candidate neoantigens in the dominant tumor clone. Although the number of validated neoantigens is similar to that in other studies, the number of candidate neoantigens is substantially lower. We used a stringent variant allele frequency of 40%; lowering this number increases the number of candidate neoantigens.

It is too early to assess the clinical importance of targeting neoantigens. Immune therapy has heretofore emphasized induction or enhancement of immune responses to tumor-associated antigens such as HER2, MUC1, mammaglobin-A, and others (38, 39). Although clinical responses have been observed with vaccines targeting tumor-associated breast cancer antigens (27, 38, 40), there is also evidence for a positive correlation between the number of candidate neoantigens and patient survival (41). Perhaps targeting a combination of both types of antigens will confer the greatest clinical benefit.

Our results support targeting neoantigens using vaccine-based immunotherapy in breast cancer. Although cancer neoantigens are targets for immune checkpoint-inhibitor therapies (1, 42), we here show their concurrent value for personalized vaccine therapy, extending the results obtained in a murine sarcoma model (1). Personalized vaccine therapy may provide many of the benefits of immune checkpoint inhibitor therapy with decreased risk of autoimmunity and other severe adverse events. Finally, our studies suggest that a combination of genomic, computational, and *in vitro* functional assays can be used to identify, prioritize, and validate candidate breast cancer neoantigens, thereby facilitating clinical translation of this approach.

Disclosure of Potential Conflicts of Interest

No potential conflicts of interest were disclosed.

Authors' Contributions

Conception and design: X. Zhang, M.J. Ellis, T.P. Fleming, S.P. Goedegebuure, W.E. Gillanders

Development of methodology: X. Zhang, J.M. Herndon, S. Li, L. Li, M.J. Ellis, E.R. Mardis, T.P. Fleming, W.E. Gillanders

Acquisition of data (provided animals, acquired and managed patients, provided facilities, etc.): X. Zhang, S. Kim, J.M. Herndon, S. Li, S.D. Soysal, L. Li, T. Primeau, N. Myers, M. Sturmoski, I.S. Hagemann, M.J. Ellis, E.R. Mardis, W.E. Gillanders

Analysis and interpretation of data (e.g., statistical analysis, biostatistics, computational analysis): X. Zhang, S. Kim, J. Hundal, A.A. Petti, S.D. Soysal, C.A. Miller, S.P. Goedegebuure, W.E. Gillanders

Writing, review, and/or revision of the manuscript: X. Zhang, S. Kim, J. Hundal, M.D. McLellan, C.A. Miller, M.J. Ellis, E.R. Mardis, S.P. Goedegebuure, W.E. Gillanders

Downloaded from http://aacrjournals.org/cancerimmunores/article-pdf/5/7/516/2351349/516.pdf by guest on 18 July 2024

Administrative, technical, or material support (i.e., reporting or organizing data, constructing databases): X. Zhang, S. Kim, J. Hoog, N. Myers, T.L. Vickery, T. Hansen, W.E. Gillanders
Study supervision: X. Zhang, S. Li, W.E. Gillanders

Acknowledgments

We thank Dr. Robert Schreiber for his comments, suggestions, and support. We thank Dr. Matthew Gubin for technical advice. We thank the staff at the McDonnell Genome Institute for their expertise and support. We also thank Dr. Seth D. Crosby and Chris Sawyer from the Genome Technology Access Center for technical consultant and expertise input.

Grant Support

This work is supported by grants to W.E. Gillanders from Susan G. Komen for the Cure (KG111025), NCI T32 CA 009621, NIH P30CA091842, the Siteman Cancer Center/Barnes-Jewish Hospital Foundation Cancer Frontier Fund (BJHF CFF 7538-55), and the Siteman Cancer Center Siteman Investment Program (SIPPre-SPORE 3781).

Received October 6, 2016; revised April 6, 2017; accepted May 31, 2017; published OnlineFirst June 15, 2017.

References

1. Gubin MM, Zhang X, Schuster H, Caron E, Ward JP, Noguchi T, et al. Checkpoint blockade cancer immunotherapy targets tumour-specific mutant antigens. Nature 2014;515:577–81.
2. Hundal J, Carreno BM, Petti AA, Linette GP, Griffith OL, Mardis ER, et al. pVAC-Seq: a genome-guided in silico approach to identifying tumor neoantigens. Genome Med 2016;8:11.
3. Matsushita H, Vesely MD, Koboldt DC, Rickert CG, Uppaluri R, Magrini VJ, et al. Cancer exome analysis reveals a T-cell-dependent mechanism of cancer immunoediting. Nature 2012;482:400–4.
4. Carreno BM, Magrini V, Becker-Hapak M, Kaabinejadian S, Hundal J, Petti AA, et al. A dendritic cell vaccine increases the breadth and diversity of melanoma neoantigen-specific T cells. Science 2015;348:803–8.
5. Alexandrov LB, Nik-Zainal S, Wedge DC, Aparicio SA, Behjati S, Biankin AV, et al. Signatures of mutational processes in human cancer. Nature 2013;500:415–21.
6. Lawrence MS, Stojanov P, Mermel CH, Robinson JT, Garraway LA, Golub TR, et al. Discovery and saturation analysis of cancer genes across 21 tumour types. Nature 2014;505:495–501.
7. van Rooij N, van Buuren MM, Philips D, Velds A, Toebes M, Heemskerk B, et al. Tumor exome analysis reveals neoantigen-specific T-cell reactivity in an ipilimumab-responsive melanoma. J Clin Oncol 2013;31:e439–42.
8. Robbins PF, Lu YC, El-Gamil M, Li YF, Gross C, Gartner J, et al. Mining exomic sequencing data to identify mutated antigens recognized by adoptively transferred tumor-reactive T cells. Nat Med 2013;19:747–52.
9. Wolfel T, Hauer M, Schneider J, Serrano M, Wolfel C, Klehmann-Hieb E, et al. A p16INK4a-insensitive CDK4 mutant targeted by cytolytic T lymphocytes in a human melanoma. Science 1995;269:1281–4.
10. Li S, Shen D, Shao J, Crowder R, Liu W, Prat A, et al. Endocrine-therapy-resistant ESR1 variants revealed by genomic characterization of breast-cancer-derived xenografts. Cell Rep 2013;4:1116–30.
11. Griffith M, Griffith OL, Smith SM, Ramu A, Callaway MB, Brummett AM, et al. Genome modeling system: a knowledge management platform for genomics. PLoS Comput Biol 2015;11:e1004274.
12. Li H, Durbin R. Fast and accurate short read alignment with Burrows-Wheeler transform. Bioinformatics 2009;25:1754–60.
13. Li H, Handsaker B, Wysoker A, Fennell T, Ruan J, Homer N, et al. The sequence alignment/map format and SAMtools. Bioinformatics 2009;25:2078–9.
14. Li H. A statistical framework for SNP calling, mutation discovery, association mapping and population genetical parameter estimation from sequencing data. Bioinformatics 2011;27:2987–93.
15. Larson DE, Harris CC, Chen K, Koboldt DC, Abbott TE, Dooling DJ, et al. SomaticSniper: identification of somatic point mutations in whole genome sequencing data. Bioinformatics 2012;28:311–7.
16. Koboldt DC, Chen K, Wylie T, Larson DE, McLellan MD, Mardis ER, et al. VarScan: variant detection in massively parallel sequencing of individual and pooled samples. Bioinformatics 2009;25:2283–5.
17. Koboldt DC, Zhang Q, Larson DE, Shen D, McLellan MD, Lin L, et al. VarScan 2: somatic mutation and copy number alteration discovery in cancer by exome sequencing. Genome Res 2012;22:568–76.
18. Saunders CT, Wong WS, Swamy S, Becq J, Murray LJ, Cheetham RK. Strelka: accurate somatic small-variant calling from sequenced tumor-normal sample pairs. Bioinformatics 2012;28:1811–7.
19. Cabanski CR, Magrini V, Griffith M, Griffith OL, McGrath S, Zhang J, et al. cDNA hybrid capture improves transcriptome analysis on low-input and archived samples. J Mol Diagn 2014;16:440–51.
20. Nielsen M, Lundegaard C, Worning P, Lauemoller SL, Lamberth K, Buus S, et al. Reliable prediction of T-cell epitopes using neural networks with novel sequence representations. Protein Sci 2003;12:1007–17.
21. Lundegaard C, Lamberth K, Harndahl M, Buus S, Lund O, Nielsen M. NetMHC-3.0: accurate web accessible predictions of human, mouse and monkey MHC class I affinities for peptides of length 8–11. Nucleic Acids Res 2008; 36(Web Server issue): W509–12.
22. Hansen T, Myers N. Peptide induction of surface expression of class I MHC. Curr Protoc Immunol 2003;Chapter 18:Unit 181.
23. Stromnes IM, Schmitt TM, Chapuis AG, Hingorani SR, Greenberg PD. Re-adapting T cells for cancer therapy: from mouse models to clinical trials. Immunol Rev 2014;257:145–64.
24. Eberlein TJ, Rosenstein M, Rosenberg SA. Regression of a disseminated syngeneic solid tumor by systemic transfer of lymphoid cells expanded in interleukin 2. J Exp Med 1982;156:385–97.
25. Rosenberg SA, Restifo NP, Yang JC, Morgan RA, Dudley ME. Adoptive cell transfer: a clinical path to effective cancer immunotherapy. Nat Rev Cancer 2008;8:299–308.
26. Elvin J, Potter C, Elliott T, Cerundolo V, Townsend A. A method to quantify binding of unlabeled peptides to class I MHC molecules and detect their allele specificity. J Immunol Methods 1993;158:161–71.
27. Tiriveedhi V, Tucker N, Herndon J, Li L, Sturmoski M, Ellis M, et al. Safety and preliminary evidence of biologic efficacy of a mammaglobin-a DNA vaccine in patients with stable metastatic breast cancer. Clin Cancer Res 2014;20:5964–75.
28. Castle JC, Kreiter S, Diekmann J, Lower M, van de Roemer N, de Graaf J, et al. Exploiting the mutanome for tumor vaccination. Cancer Res 2012;72:1081–91.
29. Yadav M, Jhunjhunwala S, Phung QT, Lupardus P, Tanguay J, Bumbaca S, et al. Predicting immunogenic tumour mutations by combining mass spectrometry and exome sequencing. Nature 2014;515:572–6.
30. Zhang X, Sharma PK, Peter Goedegebuure S, Gillanders WE. Personalized cancer vaccines: Targeting the cancer mutanome. Vaccine 2017;35:1094–100.
31. Liedtke C, Bernemann C, Kiesel L, Rody A. Genomic profiling in triple-negative breast cancer. Breast Care (Basel) 2013;8:408–13.
32. Shah SP, Roth A, Goya R, Oloumi A, Ha G, Zhao Y, et al. The clonal and mutational evolution spectrum of primary triple-negative breast cancers. Nature 2012;486:395–9.
33. Ding L, Ellis MJ, Li S, Larson DE, Chen K, Wallis JW, et al. Genome remodelling in a basal-like breast cancer metastasis and xenograft. Nature 2010;464:999–1005.
34. Tran E, Turcotte S, Gros A, Robbins PF, Lu YC, Dudley ME, et al. Cancer immunotherapy based on mutation-specific $CD4^+$ T cells in a patient with epithelial cancer. Science 2014;344:641–5.
35. Kakimi K, Karasaki T, Matsushita H, Sugie T. Advances in personalized cancer immunotherapy. Breast Cancer 2017;24:16–24.
36. Schumacher TN, Schreiber RD. Neoantigens in cancer immunotherapy. Science 2015;348:69–74.
37. Verdegaal EM, de Miranda NF, Visser M, Harryvan T, van Buuren MM, Andersen RS, et al. Neoantigen landscape dynamics during human melanoma-T cell interactions. Nature 2016;536:91–5.

Downloaded from http://aacrjournals.org/cancerimmunolres/article-pdf/5/7/516/2351349/516.pdf by guest on 18 July 2024

38. Sanchez K, Page D, McArthur HL. Immunotherapy in breast cancer: An overview of modern checkpoint blockade strategies and vaccines. Curr Probl Cancer 2016;40:151–62.
39. Li L, Goedegebuure P, Mardis ER, Ellis MJ, Zhang X, Herndon JM, et al. Cancer genome sequencing and its implications for personalized cancer vaccines. Cancers (Basel) 2011;3:4191–211.
40. Clifton GT, Mittendorf EA, Peoples GE. Adjuvant HER2/neu peptide cancer vaccines in breast cancer. Immunotherapy 2015;7:1159–68.
41. Brown SD, Warren RL, Gibb EA, Martin SD, Spinelli JJ, Nelson BH, et al. Neo-antigens predicted by tumor genome meta-analysis correlate with increased patient survival. Genome Res 2014;24: 743–50.
42. Rizvi NA, Hellmann MD, Snyder A, Kvistborg P, Makarov V, Havel JJ, et al. Mutational landscape determines sensitivity to PD-1 blockade in non-small cell lung cancer. Science 2015;348: 124–8.

Downloaded from http://aacrjournals.org/cancerimmunolres/article-pdf/5/7/516/2351349/516.pdf by guest on 18 July 2024